IEEE Access
Multidisciplinary | Rapid Review | Open Access Journal

Received August 17, 2016, accepted September 14, 2016, date of publication September 20, 2016,
date of current version October 6, 2016.

Digital Object Identifier 10.1109/ACCESS.2016.2611618

Millimeter Wave Power Monitoring in EAST ECRH System

WEIYE XU, HANDONG XU, FUKUN LIU, YUNYING TANG, ZEGE WU, XIAOJIE WANG, JIAN WANG, AND JIANQIANG FENG

Institute of Plasma Physics, Chinese Academy of Sciences, Hefei, China

Corresponding author: W. Xu (xuweiye@ipp.cas.cn)

This work was supported in part by the National Magnetic Confinement Fusion Science Program of China under Grant 2011GB102000 and Grant 2015GB103000, in part by the National Natural Science Foundation of China Grant 11305210, and in part by the Science Foundation of Institute of Plasma Physics, Chinese Academy of Sciences under Grant Y45ETY230B.

ABSTRACT This paper presents a stable millimeter-wave power monitoring system for ECRH on EAST tokamak. The real-time power monitoring was realized based on power monitor miter bends. The ''Exchange'' method was proposed to monitor the reflection power for RF protection. A cRIO-based signal process unit was designed, it is robust and has the response time of 1 μs. The power monitoring system was tested and the experimental results were discussed.

INDEX TERMS ECRH, EAST tokamak, cRIO, Labview, millimeter wave power monitoring.

I. INTRODUCTION

A 140GHz electron cyclotron resonance heating system for EAST (Experimental Advanced Superconducting Tokamak, HT-7U) is being built in ASIPP (Institute of Plasma Physics, Chinese Academy of Sciences) [1], [2] It is designed to inject stable 140GHz/4MW/100s (up to 4MW/1000s in the best of circumstances) wave power to EAST. The schematic is shown in Fig.1. The ECRH system includes four gyrotrons [3] which are capable of producing 900∼1000 kW of RF output power for pulse lengths up to 1000 seconds.

Up to now, the first two gyrotrons which are shown in Fig.2 have been tested in ASIPP. In recent experimental campaign, the Gycom gyrotron oscillation of 980kW/1s, 903kW/10s, 834kW/95s and 650kW/754s were demonstrated, and the CPI gyrotron oscillation of 721kW/0.5s, 647kW/2s, 499kW/80s and 406kW/98s were demonstrated.

In EAST ECRH system, the power monitoring system is an important part of the supervisory control system. It is used to monitor the incident millimeter wave power and reflected wave power in real time, and to realize RF protection. This RF protection is implemented by comparing the voltage signal of an RF sampling diode with an adjustable reference. It removes cathode voltage and anode voltage whenever the reflected power is too high or the incident power is too low (when the gyrotron loses the correct output mode). In this study, the millimeter wave power monitoring system is designed and some important experimental results are discussed.

II. MILLIMETER WAVE POWER MONITORING METHOD

The schematic of the millimeter wave power monitoring system is shown in Fig.3. The power monitor miter bends are developed for waveguide transmission lines [4]–[6]. In EAST ECRH system, the millimeter-wave is transmitted in corrugated waveguides, the power monitor miter bends designed by GA and Gycom have been used to detect the incident waves and the reflected wave. As shown in Fig.3, Fig.4, and Fig.5, the power monitor bend will leak out a little incident RF power and reflected RF power which is received by the antennas which are connected by attenuators, detectors, amplifiers and signal processing devices successively. The amplifiers are with low noise, low offset voltage, and fast response. The detectors are based on Schottky Barrier Beam Lead Diodes because of the advantages of fast response and wide dynamic range [7]. The signal processing device is used to acquire signals in real time and compare the acquired signals with the user-defined thresholds to realize the RF protection. It will be discussed in detail in part three.

The coupling of the power monitor miter bend designed by GA from HE11 in the high-power waveguide to the output of the horn antennas is approximately 65.9 dB below the incident power. The directivity for reasonably low order modes is typically better than 20dB. And the coupling of the power monitor miter bend for Gycom gyrotron is not clear, but it will not be the difficulty for us to realize the real time power monitoring as shown below.

2169-3536 © 2016 IEEE. Translations and content mining are permitted for academic research only.
Personal use is also permitted, but republication/redistribution requires IEEE permission.
See http://www.ieee.org/publications_standards/publications/rights/index.html for more information.

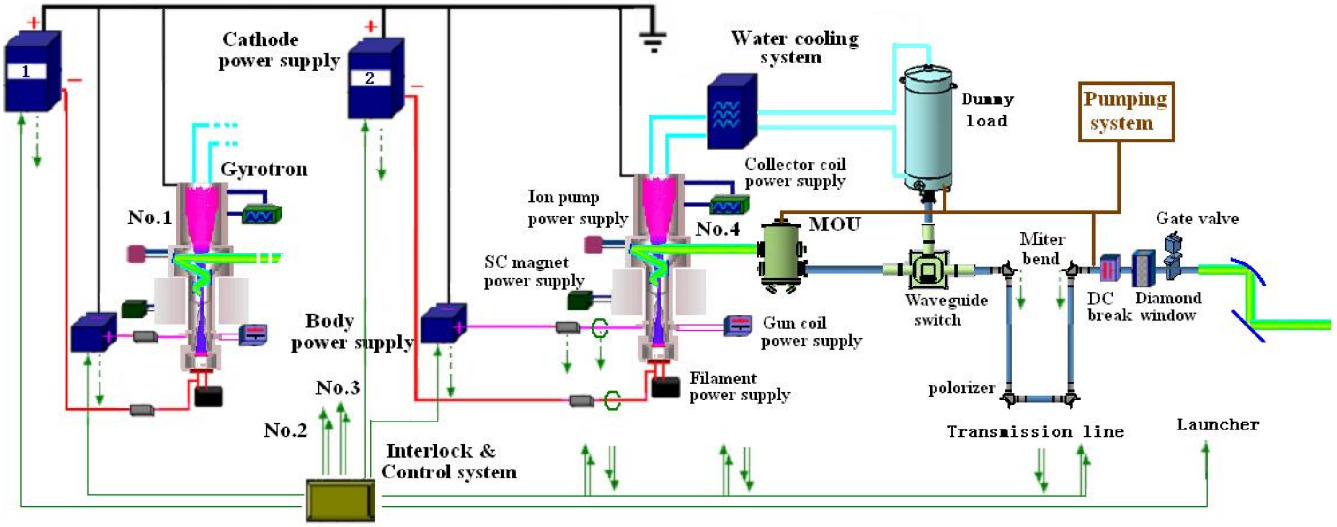

FIGURE 1. Schematic of the ECRH system. It consists of gyrotron subsystem, transmission subsystem, antenna subsystem, supervisory control subsystem, data acquisition and power measurement subsystem, power supply subsystem, water cooling subsystem, etc.

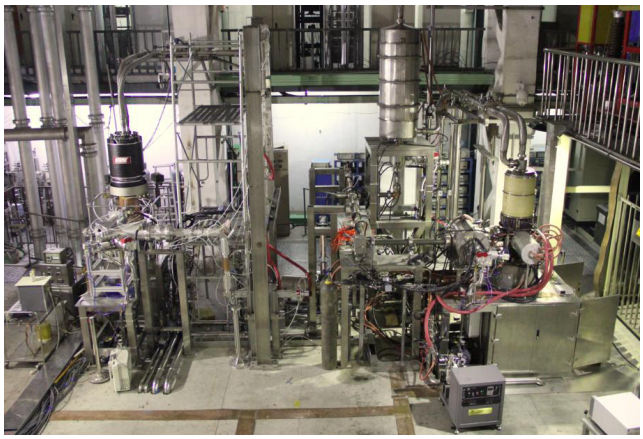

FIGURE 2. The picture of the wave sources of first 2MW ECRH system in ASIPP. The two gyrotrons are manufactured by CPI and Gycom, respectively.

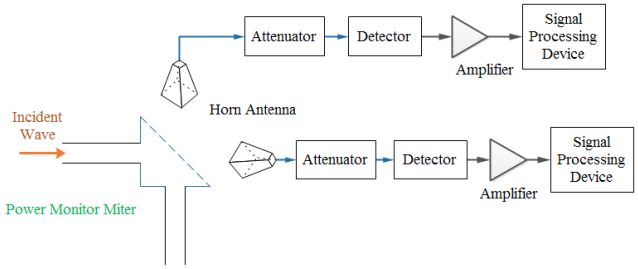

FIGURE 3. Schematic of millimeter wave power monitoring system. The detector transforms the wave power into voltage signal according to the sensitivity curve of the detector. The amplifier makes the voltage signal big enough to be measured by the signal processing device.

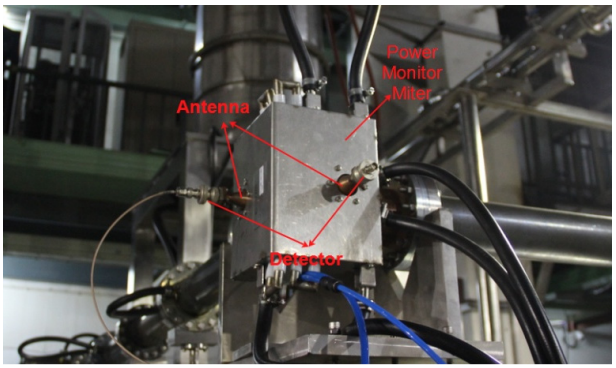

FIGURE 4. Photo of the power monitor miter bend, antennas, and detectors for Gycom gyrotron.

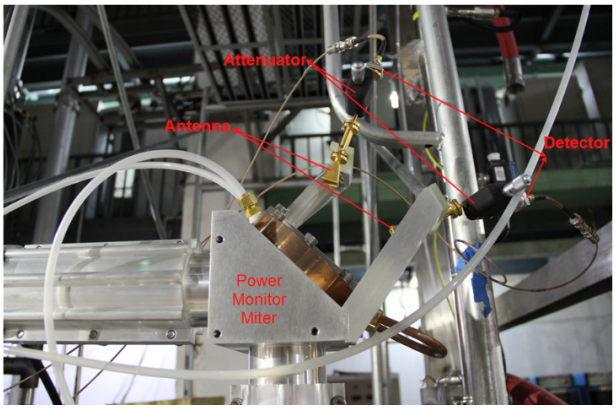

FIGURE 5. Photo of the power monitor miter bend, antennas, attenuators, and detectors for CPI gyrotron. The power monitor miter bend is designed by GA.

A. INCIDENT WAVE POWER MONITORING

The 3D pictures of the power test benches for Gycom gyrotron and CPI gyrotron are shown in Fig.6 and Fig.8. One power monitor is situated between the MOU and the dummy load for CPI gyrotron. This power monitor miter bend is situated before the polarisers and it picks up only

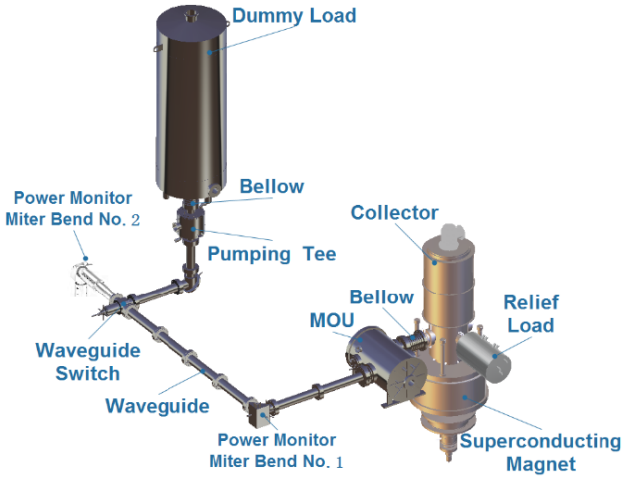

FIGURE 6. Power test bench of the Gycom gyrotron. The gyrotron output power is the sum of the power of dummy load, bellows, waveguides, waveguide switch, MOU, miter bend, and output window. Two power monitor miter bends are used. One power monitor miter is situated between MOU and dummy load, the other one which is similar to the one used for CPI gyrotron is situated between the first power monitor bend and tokamak. The gyrotron output power can be got by calorimetric method.

one polarisation. The output wave from the MOU is H-plane linearly polarised.

As shown in Fig.6, two power monitors are used for Gycom gyrotron. One is situated between the MOU and the dummy load, the other one which is similar to the one used for CPI gyrotron is situated between the first power monitor miter bend and tokamak. Both two power monitors pick up only one polarisation, and both are situated before the polarisers. The output wave from the MOU is E-plane linearly polarised for No.1 power monitor miter bend, and thus the wave is H-plane linearly polarised for No.2 power monitor miter bend. The millimeter wave in all power monitors are with the desired polarisation.

The power monitor miter bends are calibrated by calorimetric method. The relationship between the detector output voltage and RF output power can be found by analyzing the data of detector output voltage and gyrotron output power got by calorimetric method. The calorimetric method got the gyrotron output power by measuring the difference of the water temperature between the outlet and the inlet of each water cooling circuit (such as dummy load, MOU, and etc.). In our system, after temperature calibration, the power measurement error is caused mostly by the resolution of temperature transmitter and the accuracy of the flow meter. The power is calculated by,

$$P_{real} = \frac{C \cdot F}{\tau} \int_{t_1}^{t_n=t_1+\tau+60} [Tout\ (t) - Tin\ (t)]\, dt \qquad (1)$$

where Tout(t) is the outlet temperature of the water cooling circuit, Tin(t) is the inlet temperature, t1 is the pulse start time, τ is pulse duration. Tin(t) is controlled to be stable in experiments, can be seen as a constant approximately. Because 60s after the end of the pulse, the temperature difference will decrease gradually to zero, so the integral time is set as $(\tau + 60)$. Assume,

$$T = \int_{t_1}^{t_n=t_1+\tau+60} [Tout\ (t) - Tin\ (t)]\, dt \qquad (2)$$

In the worst case, the relative error of measured power is

$$\begin{aligned}\delta_{power} \approx \pm \Bigg[&\left| \frac{\partial \ln (P_{real})}{\partial F} \Delta F \right| + \left| \frac{\partial \ln (P_{real})}{\partial T} \Delta T \right| \\ &+ \left| \frac{\partial \ln (P_{real})}{\partial \tau} \Delta \tau \right| + \left| \frac{\partial \ln (P_{real})}{\partial C} \Delta C \right| \Bigg] \\ = \pm &\left(\left| \frac{\Delta F}{F} \right| + \left| \frac{\Delta T}{T} \right| + \left| \frac{\Delta \tau}{\tau} \right| + \left| \frac{\Delta C}{C} \right| \right) \qquad (3)\end{aligned}$$

where ΔF, ΔT, $\Delta \tau$ is the absolute error of flow, temperature integral, wave-output duration respectively. In our system,

$$\left| \frac{\Delta F}{F} \right| \approx \frac{F_{full}}{100F} \qquad (4)$$

$$\Delta \tau \approx 2\ ms = 0.002\ s \qquad (5)$$

$$\left| \frac{\Delta T}{T} \right| \approx \frac{0.02 \cdot (\tau + 60)}{\max(\tau, t_r) \cdot T_{max}} \qquad (6)$$

where F_{full} is the set full flow, T_{max} is the maximum of the difference between final and initial water temperatures in each circuit, t_r is the duration when temperature difference rise from zero to maximum (It is related to the response time of temperature transmitter, the character of dummy load and the pulse duration). As shown in Fig.7,

$$T \approx \max(\tau, t_r) \cdot T_{max} \qquad (7)$$

Because the temperature error is 0.02 °C,

$$\Delta T \approx 0.02 \cdot (\tau + 60) \qquad (8)$$

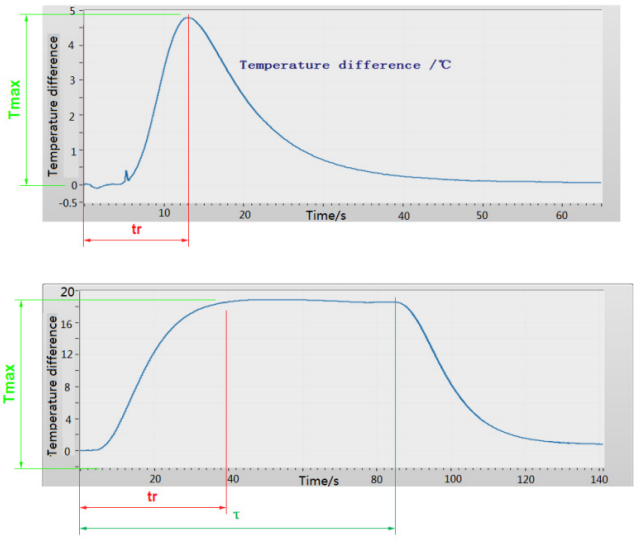

FIGURE 7. Temperature difference between outlet and inlet of dummy load cooling circuit. The figure above shows the situation when tr is bigger than τ. The figure bellow shows the situation when tr is smaller than τ.

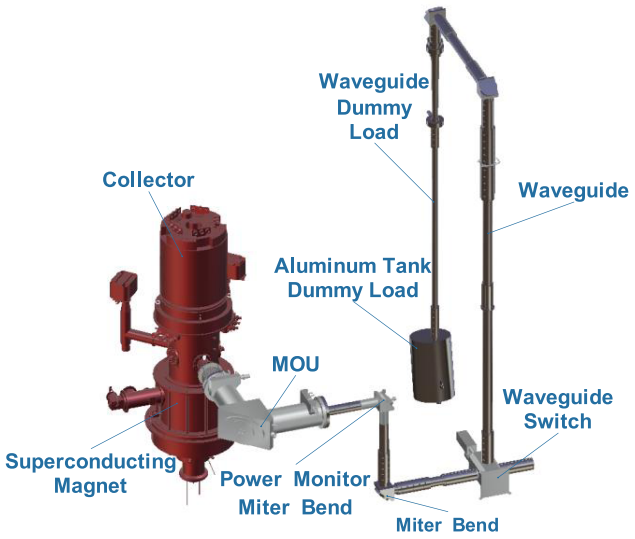

FIGURE 8. Power test bench of the CPI gyrotron. The gyrotron output power is the sum of the power of waveguide dummy load, aluminum tank dummy load, bellows, waveguides, waveguide switch, MOU, miter bends, and output window.

We set the specific heat capacity of water as,

$$C = 4.18\ \text{kJ}/(\text{kg} \cdot \text{K}) \tag{9}$$

But actually, the specific heat capacity will change along with the temperature and the pressure, the maximum relative error is,

$$\left|\frac{\Delta C}{C}\right| = \frac{4.217 - 4.18}{4.217} \times 100\% \approx 0.88\% \tag{10}$$

So, the maximum calorimetric measurement error is,

$$\delta_{power} \approx \pm\left(\frac{F_{full}}{F} + \frac{2 \cdot (\tau + 60)}{\max(\tau, t_r) \cdot T_{max}} + \frac{0.2}{\tau} + 0.88\right)\% \tag{11}$$

where F is the volume flow of water in each circuit, for instance, F is about 42 m^3/h and the F_{full} is set as 100 m^3/h for Gycom Dummy load. T_{max} is the maximum of the difference between final and initial water temperatures in each circuit, t_r is the duration when temperature difference rise from zero to maximum, τ is wave-output duration. And all parameters are in standard international unit. When the gyrotron pulse duration is bigger than 1s, the relative error of calorimetric measurement is less than 10% and less than 5% in most cases.

We can change the gyrotrons output power by changing the cathode voltage, anode voltage, filament power, and superconducting magnet current. For Gycom gyrotron, when the waveguide switch makes the RF wave power transmitted to dummy load, the voltage output by No.1 power monitor can be measured, and the output power can be got by calorimetric method. Then keep the same cathode voltage, anode voltage, and etc., and make waveguide switch transmit the RF wave to tokamak, the voltage output by No.2 power monitor can be got. For CPI gyrotron, there is only one power monitor, and the operation is similar to that of the No.1 power monitor for Gycom gyrotron. Several sets of data about the gyrotron output power and the detector voltage of incident wave were got when the gyrotrons were tested. The function about the voltage and the output power was got by curve fitting. It will be presented in section four.

B. REFLECTED WAVE POWER MONITORING

Whereas the forward power is transmitted mainly in the HE_{11} mode with known coupling at the miter bend power detector, reflections appear in mode mixtures including high order modes which can have different coupling factors. Hence the coupling measurement of reflected waves will only be a rough approximation to the coupling in such a case.

The 'Exchange' method is used to measure the reflected wave power because we don't have the 140GHz band instruments like millimeter wave source, millimeter power meter, or network analyzer, etc. to measure the real insertion loss of attenuators and the sensitivity of detectors.

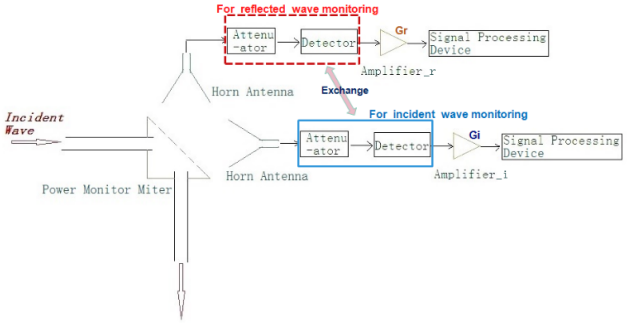

FIGURE 9. Normal configuration for gyrotron test.

Firstly, we assume that the reflected power has the same coupling factor with the forward power. In the normal operation, the configuration for gyrotron test is shown in Fig.9. The characteristic of the attenuator and detector for incident wave monitoring can be got by comparing the power data using calorimetric method which have been discussed above. In the power monitoring link, actually, the couplings of the power monitor miter bend for incident wave and reflected wave are approximately equal. The antennas have almost the same gain. The amplifiers are linear with adjustable known amplification factor. That is, only the attenuator-detector characteristic is not clear. As shown in Fig.10, in order to measure the characteristic of the attenuator-detector for reflected wave monitoring, the attenuator-detector for reflected wave monitoring and the attenuator-detector for incident wave monitoring are exchanged. In this configuration, the attenuator-detector for reflected wave is used to monitor the incident wave power which is measured by calorimetric method. Assume the amplification factor of the amplifier for reflected wave monitoring is Gr, the amplification factor of the amplifier for incident wave monitoring is Gi,

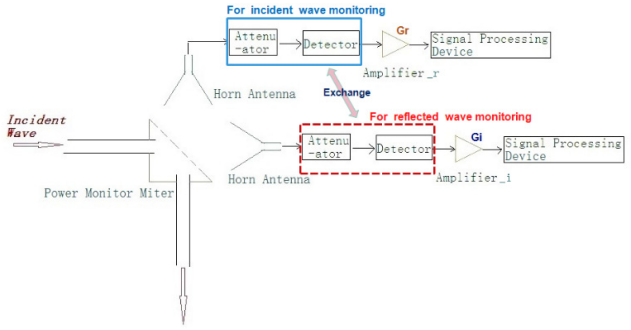

FIGURE 10. Configuration for measuring the characteristic of the attenuator-detector for reflected wave monitoring. The attenuator-detector for incident wave monitoring and the attenuator-detector for reflected wave monitoring are exchanged.

and after gyrotron test in configuration shown in Fig.10, we got the function, $V_i = f(p_i)$, where Vi is the voltage outputted by amplifer_i, p_i is the output power of gyrotron. Then, in normal configuration shown in Fig.9, the voltage outputted by amplifier_r will be, $V_r = \frac{G_r}{G_i} \cdot f(p_r)$, where p_r is the reflected power. So, the reflected power is,

$$P_r = f^{-1}(\frac{G_i}{G_r} \cdot V_r) \tag{12}$$

where the unit of P_r is Watt.

So, the reflected power can be got roughly by,

$$P_{rr} = 10\lg(P_r) = 10\lg\left(f^{-1}(\frac{G_i}{G_r} \cdot V_r)\right) \tag{13}$$

where the unit of P_{rr} is dBW.

III. SIGNAL PROCESSING UNIT

The architecture of the signal processing unit is presented in Fig.11. The signal processing unit is based on the CompactRIO (cRIO) [8] platform and Labview. The cRIO device and the center console are placed in heating device room near to gyrotrons. The center console is used to control the timing sequence of operation of gyrotrons and to send the anode start-stop signal to cRIO analog I/O module. The signals output by amplifiers which are shown in part two are received by Simultaneous Analog Input C Series Module NI 9223 at a sample rate up to 1MS/s/channel.

The FPGA in cRIO chassis is programmed to realize data acquisition and RF protection. A user-controlled I/O sampling, is used to read the I/O data from the I/O items. If the disruption occurs (i.e. incident wave power is too low) or the reflected power is too high, the Digital IO C Series Module NI 9401 will send the fault signal (TTL low level signal) to anode power source and cathode power source to shut them down. Once a fault signal is generated, this fault signal will remain active for hundreds of milliseconds to make the protection more reliable.

RF protection can be set to run continuously in experiment period. But electromagnetic interference may be generated at the moment of the anode power source starts. And the interference may make the reflected signals increase too high to trigger the RF protection by mistake. The waveforms in Fig.12 show an instance. In order to solve this problem, the reflection protection is set to be ineffective until the anode voltage is bigger than a threshold (15kV is appropriate for our ECRH system).

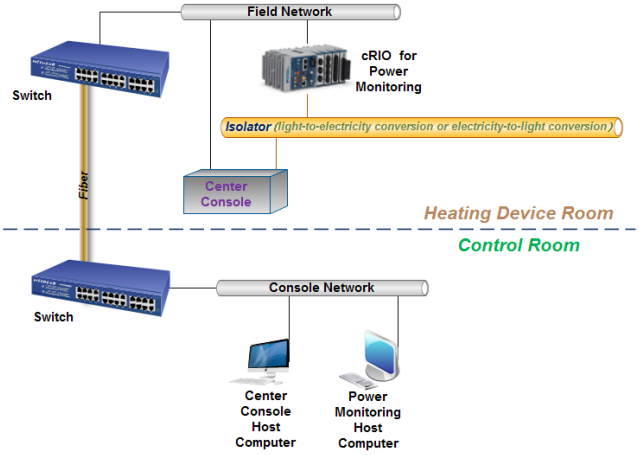

FIGURE 11. The architecture of the millimeter wave power monitoring system.

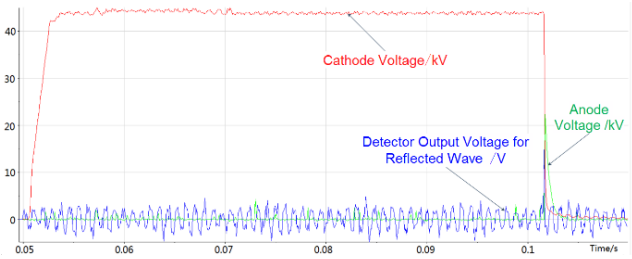

FIGURE 12. Waveforms acquired when high reflection protection happened. The moment when the anode power source started, the electromagnetic interference made the reflected wave signals increase to shut down the power sources.

IV. TEST AND EXPERIMENTAL RESULTS

A. SYSTEM TEST

The millimeter wave power monitoring system has been tested in order to insure that it is reliable and robust.

Firstly, the amplifier is tested. A signal generator and an oscilloscope are used to test the response time of the amplifier. All instruments are driven by a Labview program.

Secondly, the cRIO device is tested. Fig.13 shows the architecture of NI 9401 digital IO propagation delay test. The signal generator generates the step signal to DI port and oscilloscope. The FPGA VI which is shown in Fig.14 has been compiled and download to FPGA. The DO port will output a high level digital signal when the rising edge of DI is detected. The oscilloscope is triggered by the DO signal. Test result is shown in Fig.15, the length of time which starts when the signal input to DI port just start changing, to the time

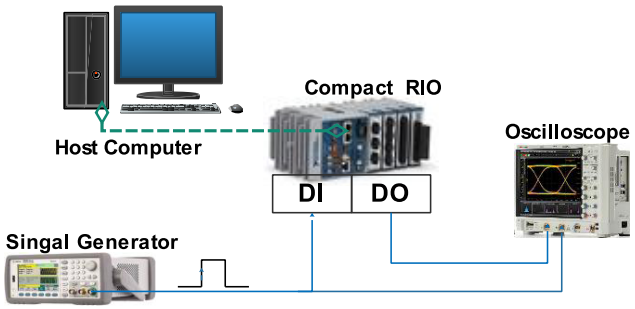

FIGURE 13. Architecture of igital I/O propagation delay test.

that the output signal reach 50% of its final output level is about 98 ns. Actually, the time for the input signal to reach 50% of its final level when the input signal starts changing is about 5ns. That is, the time required for the output to reach 50% of its final output level when the input changes to 50% of its final input level is about 93ns.

The other characteristics of cRIO have been tested also. The NI 9223 analog input sampling rate can be up to 1 MS/S/s when the Top-Level Clock is 80MHz. The NI 9401 digital input signal switching frequency can be up to 50 MHz (50 MHz square signal can be detected) with one input signal and 18 MHz (18 MHz square signal can be detected) with eight input signals. The NI 9401 digital output signal switching frequency can be up to 40 MHz (40 MHz square signal can be outputted) with one 1 MΩ, 16 pF load.

Thirdly, the RF protection function is tested. Step signals are input to analog input ports to simulate the incident voltage signal and reflected voltage signal to test the response time. The Top-Level Clock is set as 80MHz. When the analog input sampling rate is set to 1 MS/s, the response time is about 1 μs.

Fourthly, the coupling between the host computer and cRIO is tested. We shut down the host computer on purpose while the power monitoring system is working normally, then test the RF protection function. Test results shows that the RF protection is robust, and is independent of the running state of host computer.

Last but not least, the stability of this system is tested. The millimeter wave power monitoring system has been tested uninterrupted for several days at 1 MS/s sampling rate, its stability is verified.

B. EXPERIMENTAL RESULTS

The relationship between detector output voltage with gyrotron output power can be got by analyzing the data of detector output voltage and gyrotron output power. Because the longer pulse the more accurate calorimetric measurement results can be got. For getting more accurate results, all these data are got when the gyrotron pulse duration is bigger than 1s. And we found that the detector output voltage is approximately linear with RF output power of CPI gyrotron, which is shown in Fig.16. The RF output power can be expressed by a linear function,

$$P_{out} \approx 6.71 + 174.78 * V_{detctor} \tag{14}$$

The Adj. R-Square (Degree-of-freedom adjusted coefficient of determination) [9] is about 0.988. The detector voltage can express the gyrotron output power well.

However, in current configuration, the RF power generated by Gycom gyrotron is not linear with the detector output voltage of No.1 power monitor. As shown in Fig.17, the RF output power can be expressed by an exponential function,

$$P_{out} = 1155.3 - 1242.8 * \exp(-1.06 * V_{detctor}) \tag{15}$$

The Adj. R-Square [10] is about 0.576. The exponential function can represent the relationship between the RF output power and the detector output voltage to some extent. But the dispersion is large which may due to the characteristic of sensitivity of detector being vulnerable to the temperature. And actually, the varying of mode purity at the output of the MOU could cause such a scatter.

For confirming whether the power monitor or the gyrotron is to blame for the scatter, the other power monitor which is similar to the one used for CPI gyrotron is used for Gycom gyrotron. As shown in Fig.6, it is situated between the first power monitor miter bend and tokamak. Firstly, the pulse is injected to dummy load, so we can get the output power by calorimetric method. Then we keep all the same gyrotron operation parameters but inject the pulse to plasma,

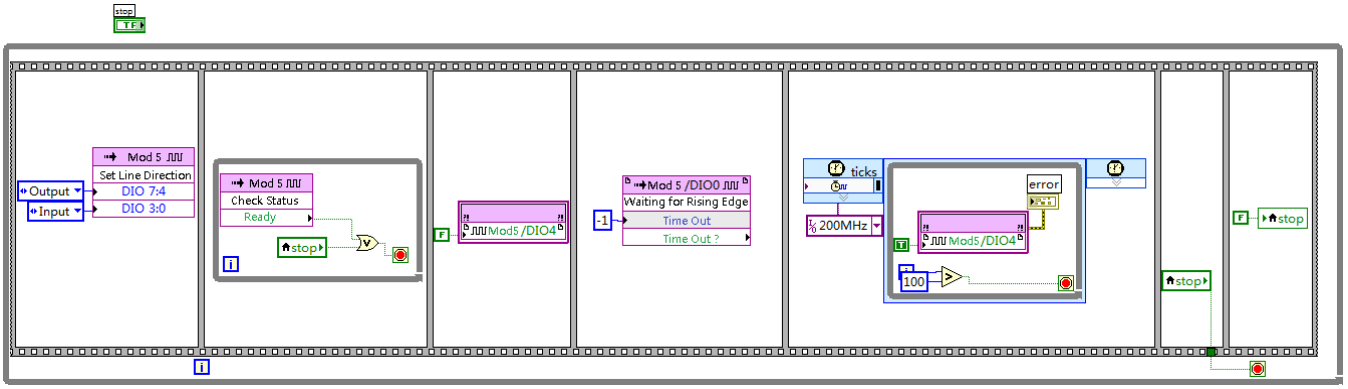

FIGURE 14. FPGA VI for digital I/O propagation delay test. 200 MHz derived clock is set as the Top-Level Clock.

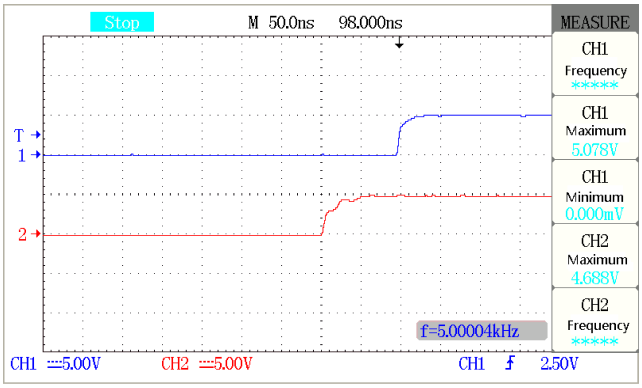

FIGURE 15. Digital I/O propagation delay test result. CH2 shows the input signal, CH1 shows the output signal. The length of time which starts when the signal input to DI port just start changing, to the time that the output signal reach 50% of its final output level is about 98 ns.

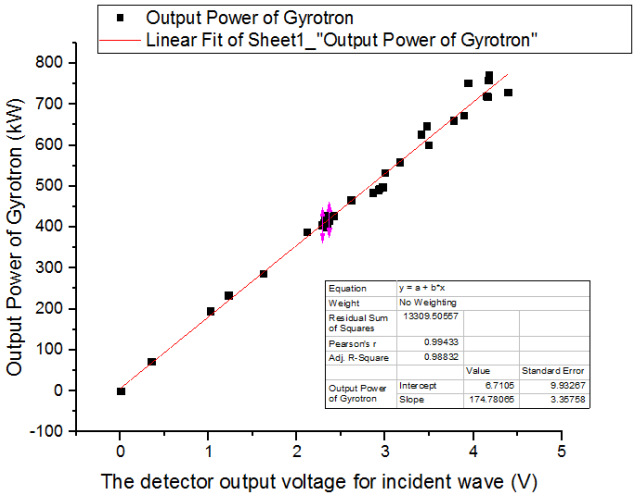

FIGURE 16. RF power generated by CPI gyrotron as a function of detector output voltage.

got the output voltage of the No.2 power monitor for Gycom gyrotron. The test results are shown in Fig.18. The RF output power can be expressed by a linear function,

$$P_{out} \approx 17.29 + 236.49 * V_{detctor} \tag{16}$$

The Adj. R-Square is about 0.961. Comparing this result with that of the No.1 power monitor, we can find that the large scatter in the signal from the Gycom No.1 power monitor is due to the power monitor, rather than the mode purity. And the large scatter is likely due to the characteristic of sensitivity of detector which is vulnerable to the temperature. We have done some experiments to verify it. We found that the RF power is approximate linear with the detector voltage when the pulse is short, and when the environment temperature is stable at the same time. But when the pulse becomes longer, the temperature of the detector will increase, we found that the scatter becomes bigger. And when the environment temperature changes, the scatter becomes bigger also. Maybe there are the other reasons to make the big scatter, they are not clear now.

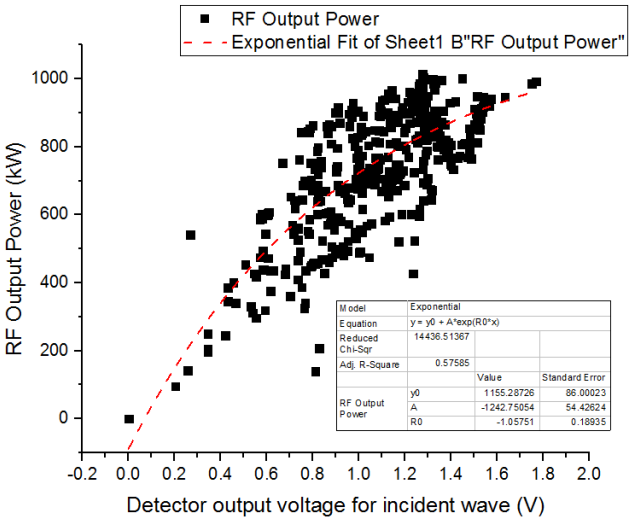

FIGURE 17. RF power generated by Gycom gyrotron as a function of detector output voltage of No.1 power monitor.

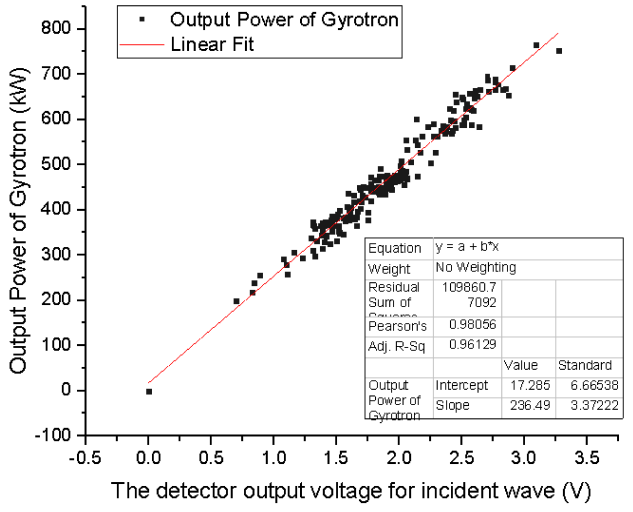

FIGURE 18. RF power generated by Gycom gyrotron as a function of detector output voltage of No.2 power monitor.

Fig.19 shows a typical detector output voltage signals for CPI gyrotron when the RF wave is transmitted to dummy load. The signal is got when the cathode voltage is −57kV, the anode voltage is 20 kV, the upper main magnetic current is 52.25 A, the lower main magnetic current is 44.54 A. And the output power is about 419 kW. The signal is ten times magnified. As we can see, when the wave power is zero, the incident voltage signal has a baseline noise whose maximum is less than 0.075 V. So, we can use 0.1 V as the minimum allowed incident detector voltage for protection. And the reflected voltages are less than 0.8 V in normal situation. We use 2 V as the maximum allowed reflected detector voltage for protection. Fig.20 shows a typical detector output voltage signals of No.1 power monitor for Gycom gyrotron when the RF power is transmitted to tokamak. This power monitor

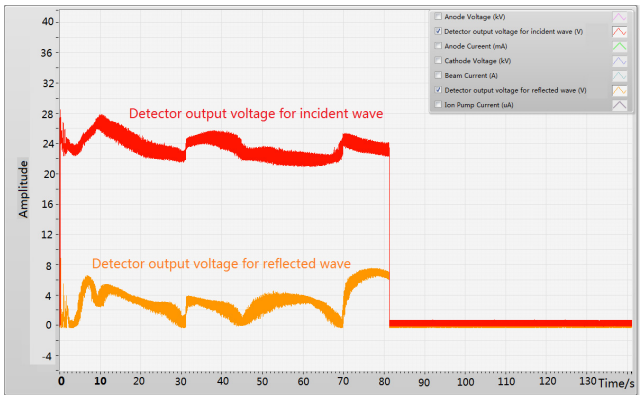

FIGURE 19. A typical detector output voltage signals for CPI gyrotron when the RF power is transmitted to dummy load.

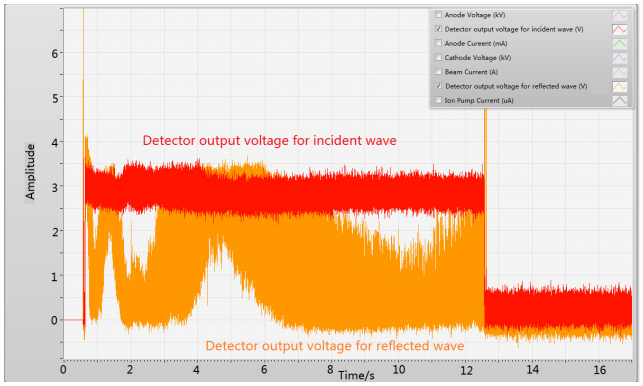

FIGURE 20. A typical detector output voltage signals for GYCOM gyrotron when the RF power is transmitted to tokamak.

is used because it is the only choice whenever the pulse is injected to dummy load or tokamak in our system at now. Although the scatter is large, but it is no problem to use it for RF protection. The signal is got when the cathode voltage is −43kV, the anode voltage is 20 kV, the main magnetic current is 50.4 A. And the output power is about 487 kW. The signal is ten times software magnified. Because we use 400 times fixed amplification at now, so the signal is small. But it can still work normally and effectively. As we can see, when the wave power is zero, the incident voltage signal has a baseline noise whose maximum is less than 0.09 V. So, we can use 0.12 V as the minimum allowed incident detector voltage for protection. And the reflected voltages are less than 0.5 V in normal situation. We use 2 V as the maximum allowed reflected detector voltage for protection.

V. CONCLUSION

Electron cyclotron resonance heating (ECRH) is one of the important heating methods for magnetic confinement fusion. A robust millimeter wave power monitoring system for ECRH on EAST tokamak was established to realize the RF protection and the real-time monitoring of gyrotron output power. It monitors the incident wave power and the reflected power in real time, shuts down cathode power supply and anode power supply whenever the reflected power is too high (high reflection happens) or the incident power is too low (disruption happens, i.e., the gyrotron loses the correct output mode) to protect the ECRH system from being damaged. The power monitoring method was presented. The 'Exchange' method was proposed to monitor the reflection power. But the measurement of the reflection power is a rough approximation because of the reflections appear in mode mixtures including high order modes. A cRIO based signal process unit was described in detail, it is robust and has 1 μs response time when the Analog Input Sampling Rate is set as 1 MS/s. The power monitoring system was tested and some experimental results were presented. The detector output voltage is approximately linear with RF output power of CPI gyrotron with higher coefficient of determination. And, wave power generated by Gycom gyrotron can be expressed by an exponential function, but with lower coefficient of determination, may due to the sensitivity of detector being vulnerable to the temperature.

ACKNOWLEDGMENTS

The authors greatly appreciate the experts from GA, CPI and GYCOM for the cooperation in the development of ECRH project on EAST.

REFERENCES

[1] X. J. Wang *et al.*, "Status of ECRH project on EAST Tokamak," in *Proc. Radiofreq. Power Plasmas, AIP Conf.*, 2014, pp. 538–541.
[2] X. Wang *et al.*, "Progress of high power and long pulse ECRH system in EAST," *Fusion Eng. Design*, vols. 96–97, pp. 181–186, Oct. 2015.
[3] V. A. Flyagin and G. S. Nusinovich, "Gyrotron oscillators," *Proc. IEEE*, vol. 76, no. 6, pp. 644–656, Jun. 1988.
[4] H. Nakamura *et al.*, "Optimization of a corrugated millimeter-wave waveguide and a miter bend by FDTD simulation," *J. Phys., Conf. Ser.*, vol. 410, no. 1, p. 012046, 2013.
[5] J. Ruiz, W. Kasparek, C. Lechte, B. Plaum, and H. Idei, "Numerical and experimental investigation of a 5-port mitre-bend directional coupler for mode analysis in corrugated waveguides," *J. Infr. Millim. Terahertz Waves*, vol. 33, no. 5, pp. 491–504, May 2012.
[6] L. Qin, Q. Zhao, and S. Z. Liu, "Design of millimeter-wave high-power power monitoring miter bend based on aperture-coupling," *Plasma Sci. Technol.*, vol. 16, no. 7, pp. 712–715, Jul. 2014.
[7] A. S. Brush, "Measurement of microwave power—A review of techniques used for measurement of high-frequency RF power," *IEEE Instrum. Meas. Mag.*, vol. 10, no. 2, pp. 20–25, Apr. 2007.
[8] National Instruments. (Jun. 7, 2016). [Online]. Available: http://www.ni.com/compactrio/whatis/
[9] OriginLab. (Jun. 7, 2016). [Online]. Available: http://www.originlab.com/doc/Origin-Help/Interpret-Regression-Result
[10] OriginLab. (Jun. 7, 2016). [Online]. Available: http://www.originlab.com/doc/Origin-Help/NLFit-Algorithm

WEIYE XU was born in Qufu, China, in 1990. He received the B.S. degree in electronic science and technology from Shandong Normal University, Jinan, China, in 2011. He is currently pursuing the Ph.D. degree in nuclear science and engineering with the University of Chinese Academy of Sciences, Beijing, China. He is currently with the Institute of Plasma Physics, Chinese Academy of Sciences, Hefei, China.

His research interests include the high power microwave heating technology for plasma, electronic technology, electromagnetic field theory, and microwave technology.

HANDONG XU was born in Yuexi, China. He received the M.S. degree in microwave engineering from the Institute of Plasma Physics, Chinese Academy of Sciences, Hefei, in 2004, and the Ph.D. degree in advanced energy engineering from Kyushu University, Fukuoka, Japan, in 2008.

He participated in the research of 4 MW 2.45 GHz and 6 MW 4.6 GHz lower hybrid current drive on EAST from 2009 to 2011. Since 2009, he has been a Senior Engineer with the Institute of plasma physics, Chinese Academy of Sciences. Since 2012, he has been involved in 140 GHz 4 MW electron cyclotron resonance heating (ECRH) system and ECRH experiments on EAST. His research interests focused on the development of high power microwave heating and current drive system and corresponding experiment study on EAST Tokamak devices.

FUKUN LIU is currently a Professor with the Institute of Plasma Physics, Chinese Academy of Sciences, Hefei, China. His research interests include microwave technology and experimental plasma physics.

YUNYING TANG is currently with the Institute of Plasma Physics, Chinese Academy of Sciences, Hefei, China. Her research interests include electromagnetic analysis.

ZEGE WU is currently with the Institute of Plasma Physics, Chinese Academy of Sciences, Hefei, China. His research interests include computer control and programming.

XIAOJIE WANG is currently an Associate Researcher with the Institute of Plasma Physics, Chinese Academy of Sciences, Hefei, China. Her research interests include microwave technology and experimental plasma physics.

JIAN WANG is currently with the Institute of Plasma Physics, Chinese Academy of Sciences, Hefei, China. His research interests include water cooling technology.

JIANQIANG FENG is currently with the Institute of Plasma Physics, Chinese Academy of Sciences, Hefei, China. His research interests include electronic technology.